Journal of Solid State Chemistry 181 (2008) 2586–2590

Contents lists available at ScienceDirect

Journal of Solid State Chemistry

journal homepage: www.elsevier.com/locate/jssc

One-dimensional inorganic arrangement in the bismuth oxalate hydroxide $Bi(C_2O_4)OH$

Murielle Rivenet *, Pascal Roussel, Francis Abraham

Unité de Catalyse et de Chimie du Solide, Equipe Chimie du Solide, UCCS UMR CNRS 8181, USTL, ENSC-B.P. 90108, 59652 Villeneuve d'Ascq Cedex, France

ARTICLE INFO

Article history:
Received 25 March 2008
Received in revised form
22 May 2008
Accepted 7 June 2008
Available online 19 June 2008

Keywords:
Bismuth hydroxide
Bismuth oxalate
Bismuth oxide precursor
Crystal structure
Layered structure

ABSTRACT

Single crystals of $Bi(C_2O_4)OH$ were obtained by the slow diffusion of Bi^{3+} cations through silica gel impregnated with oxalic acid. The structure was solved in the *Pnma* space group with $a = 6.0853(2)$ Å, $b = 11.4479(3)$ Å, $c = 5.9722(2)$ Å, leading to $R = 0.0188$ and $wR = 0.0190$ from 513 unique reflections. The bismuth coordination polyhedron is a BiO_6E pentagonal bipyramid with the lone pair E sitting at an axial vertex. The opposite axial vertex is occupied by a hydroxyl oxygen atom, which is also an equatorial corner of a neighboring BiO_6E bipyramid. The sharing of the hydroxyl oxygen atoms build $^1_\infty[BiO_5E]$ zig-zag chains running down the [100] direction. These chains are aligned in a sheet parallel to the (010) plane and are further connected through oxalate ions to form a three-dimensional arrangement. On heating, $Bi(C_2O_4)OH$ decomposes to the meta-stable quadratic β-Bi_2O_3 phase.

1. Introduction

Frequently, preparative routes involving the coprecipitation of various metals have been used in order to synthesize mixed oxide materials. The main advantages of these methods are to speed up the reaction rate and to decrease the sintering temperature, which allows improving the final product homogeneity by reducing particle sizes. In particular, oxalate coprecipitation has been successfully used for the preparation of Bi-based materials such as high-T_c superconducting phases [1–3] or bismuth titanate [4–6], tantalate [7,8] or niobate [9] ferroelectrics. Bismuth oxalates have also been used as precursors to prepare catalytically active bismuth molybdate or tungstate oxides [10,11]; nevertheless, a few crystal structures of bismuth oxalates have been reported so far.

Recently, the crystal structure determination of $Bi_2(C_2O_4)_3 \cdot 6H_2O$ and $Bi_2(C_2O_4)_3 \cdot 8H_2O$ [12,13] led to the revising of the chemical formulae, $Bi_2(C_2O_4)_3 \cdot H_2C_2O_4$ and $Bi_2(C_2O_4)_3 \cdot 7H_2O$, previously ascribed to these compounds [14]. A recent paper also reported various bismuth oxalates obtained by studying bismuth oxalate precipitation as a function of pH and temperature [15]. The reported compounds correspond to the former hexahydrate, to a heptahydrate with an hexagonal symmetry and to a hydroxy-oxalate with an orthorhombic symmetry and the chemical formula $BiOH(C_2O_4)$, corresponding to the stoichiometry previously suggested by Umabala et al. [5] for $BiO(HC_2O_4)$.

As the efficiency of crystal growth by using the slow diffusion of ions through silica gel impregnated with oxalic acid has been demonstrated for slowly soluble oxalate compounds [16], this method was applied to bismuth oxalate in an effort to expand the solid-state studies on bismuth compounds. The use of this method allowed us to isolate crystals of $Bi(C_2O_4)OH$, whose crystal structure study is herein reported together with a complete analysis of its thermal decomposition.

2. Experimental

2.1. Single-crystal synthesis, data collection and structure determination

Single crystals of $Bi(C_2O_4)OH$ are obtained using the crystal growth gel method, which is helpful for single crystals' elaboration of low soluble solids. The gel is prepared by pouring 1 M sodium metasilicate solution into a mixture of 1 M oxalic acid, further acting as a source of anions, and 3 M nitric acid so as to obtain a pH between 3.5 and 4. The resulting solution is allowed to set in tubes of internal diameter 15 mm to obtain the silica gel. Ammonium cations were substituted for Na^+ cations by ionic exchange using a nitric solution of oxalic acid 0.2 M and ammonium nitrate 2 M added onto the gel.

Pouring an aqueous solution of bismuth nitrate (0.25 M, 1 mL) mixed with ammonium nitrate (2 M, 2 mL) diluted in deionized water (4 mL) onto the set gel allows the slow diffusion of Bi^{3+} cations through the silica gel impregnated with oxalic acid. After a

* Corresponding author. Fax: +33 3 20 43 68 14.
E-mail address: Murielle.rivenet@ensc-lille.fr (M. Rivenet).

0022-4596/$ - see front matter © 2008 Elsevier Inc. All rights reserved.
doi:10.1016/j.jssc.2008.06.031

few days, this leads to the formation of transparent $Bi(C_2O_4)OH$ single crystals inside the gel.

Although ammonium cations are present in the starting medium, they are not found in synthesized bismuth hydroxy-oxalate. Indeed, crystal growth in silica gels is a quite particular method because diffusion rates, local concentrations and pH cannot be controlled. Consequently, the chemical composition of the resulting crystals often differs from the starting stoichiometric ratios of the solutions and can display some variations depending on the position within the gel.

The single-crystal diffraction intensities were measured on a BRUKER AXS SMART CCD-1K diffractometer system equipped with a Mo-target X-ray tube ($\lambda = 0.71073$ Å) operating at 2000 W power (50 kV, 40 mA). The detector was placed at a distance of 5.41 cm from the crystal. The intensities were obtained with the conditions given in Table 1 and extracted from the collected frames using the program SaintPlus 6.02 [17]. After data processing, absorption corrections were performed using a semi-empirical method based on redundancy with the SADABS program [18]. The resulting set of hkl was used for structure resolution and refinements, which were performed with the JANA2000 software package [19]. The structure was solved in the centrosymmetric *Pnma* space group. The heavy atoms were located by direct methods using SIR97 program [20], the oxygen and carbon atoms were found from successive Fourier difference maps. The atomic positions for all atoms and the anisotropic displacement parameters were included in the last cycles of refinement (Tables 2 and 3). The H atom location could not be determined because of the heavy Bi atom.

2.2. Powder synthesis and study

The $Bi(C_2O_4)OH$ powder forms at 50 °C, under constant stirring. It results from the titration of an aqueous solution of oxalic acid (0.1 M) by a solution of trivalent cations Bi^{3+} (0.1 M) acidified by nitric acid. The pH of the mixture is set at 5 by adding ammoniac (3 M). The resulting powder is filtered off, rinsed out using a mixture of deionized water and oxalic acid with pH adjusted to 5 and dried at room temperature before characterization.

Table 1
Crystal data and structure refinement for $Bi(C_2O_4)OH$

	$Bi(C_2O_4)OH$
Crystallographic data	
Formula weight ($g\,mol^{-1}$)	314.03
Crystal system	Orthorhombic
Space group	*Pnma*
Unit-cell dimensions (Å)	$a = 6.0853(2)$
	$b = 11.4479(3)$
	$c = 5.9722(2)$
Cell volume ($Å^3$)	416.05(2)
Z	4
Density, calculated ($g\,cm^{-3}$)	5.01(2)
$F(000)$	540
Intensity collection	
Wavelength (Å)	0.71069 (Mo$K\alpha$)
θ range (deg)	3.54–28.42
Data collected	$-8 \leqslant h \leqslant 7$
	$-14 \leqslant k \leqslant 15$
	$-8 \leqslant l \leqslant 7$
No. of reflections measured	2595
No. of unique reflections (all/$I > 3\sigma(I)$))	513/322
Redundancy	5.058
μ (Mo$K\alpha$) (mm^{-1})	44.65
T_{min}/T_{max}	0.739
$R(F^2)_{int}$	0.0304
Refinement	
No. of parameters	41
Weighting scheme	$1/\sigma^2$
$R(F)$ obs/all	0.0188/0.0426
w$R(F)$ obs/all	0.0190/0.0208
Max, min $\Delta\rho$($e\,Å^{-3}$)	1.78/−1.05

Table 2
Atomic coordinates and isotropic displacement parameters ($Å^2$) for $Bi(C_2O_4)OH$

Atom	Wyck.	x	y	z	U_{iso}/eq
Bi	4*c*	0.20638(6)	0.25	0.4988(2)	0.0128(2)
C	8*d*	−0.398(2)	0.5249(6)	0.937(2)	0.015(3)
O(1)	4*c*	0.054(2)	0.25	0.822(2)	0.016(2)
O(2)	8*d*	−0.396(1)	0.6296(4)	0.8881(9)	0.021(2)
O(3)	8*d*	−0.2499(9)	0.4528(5)	0.887(1)	0.018(2)

Table 3
Anisotropic displacement parameters ($Å^2$) for $Bi(C_2O_4)OH$

Atom	U_{11}	U_{22}	U_{33}	U_{12}	U_{13}	U_{23}
Bi	0.0118(2)	0.0120(2)	0.0147(2)	0	−0.0003(3)	0
C	0.013(5)	0.012(4)	0.021(5)	−0.003(3)	−0.004(3)	0.002(3)
O(1)	0.016(5)	0.018(4)	0.014(4)	0	0.007(3)	0
O(2)	0.020(3)	0.012(3)	0.030(3)	−0.001(3)	0.012(3)	0.007(2)
O(3)	0.021(4)	0.009(3)	0.023(3)	0.001(2)	0.005(2)	0.001(2)

The X-ray diffraction pattern of the as-obtained powder was recorded with a Bruker AXS D8 ADVANCE diffractometer with the parafocusing Bragg–Brentano geometry, using Cu$K\alpha_{1,}\alpha_2$ radiation ($\lambda_{K\alpha1} = 1.54051$ Å, $\lambda_{K\alpha2} = 1.54433$ Å) and an energy-dispersive detector (sol-X). The pattern was recorded under air over the angular range 5–70° (2θ), with a step length of 0.02° (2θ) and a counting time of 17 s $step^{-1}$. The powder X-ray diffraction pattern is identical to that of the theoretical pattern calculated from the crystal structure results, which evidences that a pure phase is obtained. The cell parameters of powdered $Bi(C_2O_4)OH$ refined using the JANA2000 package [19] are in good agreement with the values previously reported [15] (Table 1).

The temperature-dependent X-ray diffraction pattern was recorded using a Guinier–Lenné moving film camera. The powdered sample was deposited on the sample holder (gold grid) using an ethanol slurry, which yields, upon evaporation, a regular layer of powdered compound. The high-temperature X-ray diffraction pattern was collected in the temperature range [20–760 °C] at a heating rate of 11° h^{-1}.

Thermal gravimetric analysis and differential thermal analysis coupled to mass spectrometry (TGA/TDA/MS) were employed in order to evaluate the thermal stability of the bismuth oxalate and to investigate its decomposition behavior with increasing temperature. The thermal analyses were performed on a Setaram-coupled TGA-DTA 2-16.18 apparatus. Analyses were undertaken in air, in the temperature range 20–800 °C, at a heating rate of 300° h^{-1}, in platinum crucibles. The gases produced upon thermal treatment were collected at atmospheric pressure by means of a steel capillary line connected to the thermobalance outflow. The H_2O and CO_2 signals were measured using an on-line Pfeiffer Omnistar mass spectrometer controlled by the Quadstar 32-bit software and by monitoring $m/e = 44$ (for CO_2) and 18 (H_2O).

3. Results and discussion

3.1. Structure description

The unique bismuth atom is surrounded by eight oxygen atoms, forming a bicapped trigonal prism according to the criterion of Haigh [21]. In this polyhedron, the average Bi–O

distance is 2.512(6) Å, in agreement with the values generally observed for eight-coordinated bismuth in oxides as, for example, in $BiSbO_4$ (2.55(2) Å) [22] but larger than the values calculated for eight-coordinated bismuth atom in oxalates (i.e. 2.441(5) Å in $KBi(C_2O_4)_2 \cdot 5H_2O$ [23], 2.450(8) Å in $NH_4Bi(C_2O_4)_2 \cdot 5H_2O$ [24], 2.473(5) and 2.468(5) Å for Bi(1) and Bi(2), respectively, in $[NH(C_2H_5)_3][Bi_2(C_2O_4)_5]$ [25]). In the title compound, the Bi–O distances are spread over a large range from 2.140(7) to 2.928(6) Å (Table 4). The two shortest distances (2.140(7) and 2.372(7) Å) involve hydroxyl oxygen atoms. The four intermediate distances equivalent to 2.434(6) Å (2*x*) and 2.431(6) Å (2*x*) correspond to bismuth bonding with oxygen atoms belonging to two oxalate ions, which act as bidentate. These six bonds can be considered as "primary bonds" whereas the two longest Bi–O distances (2.928(6) Å (2*x*)) involving O(2) oxygen atoms of oxalate ions of a neighboring entity can be considered as "secondary bonds". In this compound, the division between primary and secondary bonds is clear, and only the primary bond type has to be considered in the bismuth bonding sphere. Then the bismuth atom can be seen as one-sided with six oxygen atoms forming a pentagonal pyramid. The bismuth atom is shifted from the mean basal plane in the direction opposite to the apical hydroxyl oxygen (Fig. 1). This umbrella-like environment with all Bi–O bonds on the same side of the central Bi atom may be explained to be due to the stereochemical activity of the Bi^{3+} lone pair (E), which is expected to be located opposite to the apical bond to form a pentagonal bipyramid BiO_6E. This hypothesis was confirmed by lone-pair calculation using the program Hybrid [26]. It is noticeable that in the bismuth oxalates [12,13,23–25] characterized up to now, the bismuth atoms coordination spheres are rather regular with intermediate Bi–O distances varying in a narrow range. The shorter average Bi–O distances evidenced in these compounds compared to those found in $Bi(C_2O_4)OH$ are explained by non-stereochemically active lone pairs. Although stereochemical activity of a lone electron pair has already been reported in oxalates as, for example, in the Sn compound $Sn(C_2O_4)$ [27], it is herein reported for the first time in bismuth oxalates.

The BiO_6E pentagonal bipyramids are connected via shared oxygen hydroxyl atoms leading to $^1_\infty[BiO_5E]$ zig-zag chains running down the [100] direction (Fig. 1). Parallel chains are connected by weak Bi–O(2) bonds so as to form inorganic $^2_\infty[BiO_5]$ layers parallel to the (010) plane. The chains and, by consequence the $^2_\infty[BiO_5]$ layers, are further connected through bis-bidentate oxalate ions to form a three-dimensional inorganic–organic arrangement (Fig. 2).

Considering or not the two weak Bi–O(2) bonds, the calculated valence bond sums for Bi are 3.09 and 2.89 v.u., respectively. These two values are acceptable. Calculations resulted in 2.10 and 1.91 v.u. for O(2) and O(3), respectively, whereas a valence bond sum of 1.32 v.u. was found for O(1). This value is in good agreement with the values of 1.25 and 1.40 v.u. previously reported for the hydroxyl oxygen in bismuth hydroxynitrates [28,29].

A good way to describe metal oxalate hydroxide structures is to consider metal oxalate arrangement further connected by hydroxyl oxygen sharing [30]. In our compound, the BiO_6E pentagonal bipyramids are connected through bis-bidentate oxalate ions to

Table 4
Selected interatomic distances (Å) for $Bi(C_2O_4)OH$

Bi–O(1)	2.140(7)	C–O(3)	1.26(1)
Bi–O(1)^{i}	2.372(7)	C–O(2)	1.23(1)
Bi–O(3)^{i}	2.434(6)		
Bi–O(3)^{ii}	2.434(6)	C–C^{viii}	1.56(2)
Bi–O(2)^{iv}	2.431(6)		
Bi–O(2)^{v}	2.431(6)		
Bi–O(2)^{iii}	2.928(6)		
Bi–O(2)^{vi}	2.928(6)		

(i) 1/2+*x*, *y*, 3/2−*z*, (ii) 1/2+*x*, 1/2−*y*, 3/2−*z*, (iii) −*x*, 1−*y*, 1−*z*, (iv) −1/2−*x*, 1−*y*, −1/2+*z*, (v) −1/2−*x*, −1/2+*y*, −1/2+*z*, (vi) −*x*, −1/2+*y*, 1−*z*, (vii) *x*, 1/2−*y*, z, (viii) 1−*x*, 1−*y*, 2−*z*.

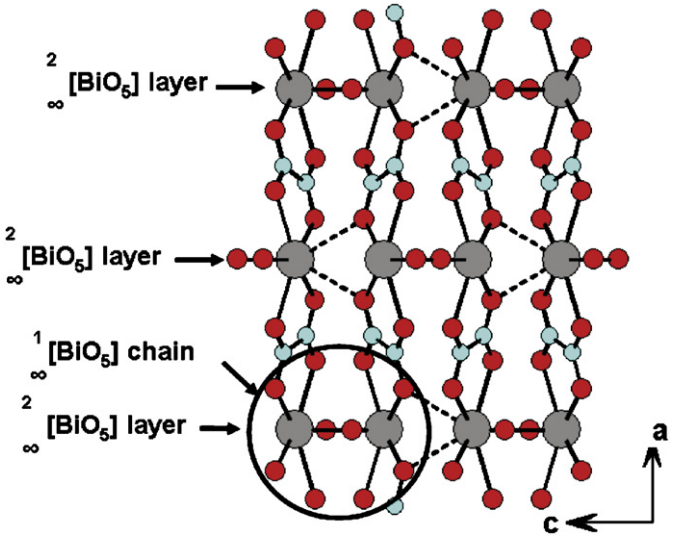

Fig. 2. Parallel $^1_\infty[BiO_5E]$ chains linked by the weak Bi–O(2) bonds to form a $^2_\infty[BiO_5]$ layer parallel to the (010) plane. The $^2_\infty[BiO_5]$ layers are connected through bis-bidentate oxalate ions to form a three-dimensional inorganic–organic arrangement.

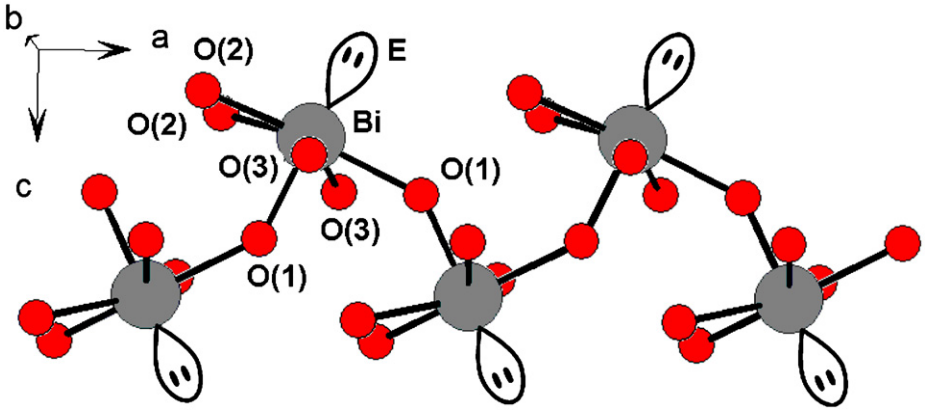

Fig. 1. The BiO_6E pentagonal bipyramids are connected via shared oxygen hydroxyl atoms to form $^1_\infty[BiO_5E]$ zig-zag chains running down [100].

form $^1_\infty$[Bi(OH)$_2$E(C$_2$O$_4$)] chains running down the [010] direction (Fig. 3a) with lone pairs alternating above and below the mean plane of the chains. The chains are connected through the two hydroxyl oxygen atoms to build the three-dimensional arrangement. The $^1_\infty$[{Bi(OH)E}(OH)(C$_2$O$_4$)] chains are similar to the $^1_\infty$[{UO$_2$}(H$_2$O)(C$_2$O$_4$)] and $^1_\infty$[{UO$_2$}(OH)(C$_2$O$_4$)] chains observed in [{UO$_2$}(H$_2$O)(C$_2$O$_4$)]·2H$_2$O [31] and M[{UO$_2$}$_2$(OH)(C$_2$O$_4$)$_2$]·2H$_2$O, M = NH$_4^+$, Na$^+$, K$^+$ [32–34] (Fig. 3b). In the uranyl oxalates, the apical oxygen atoms of the pentagonal bipyramids have their valence bonds practically satisfied by the U=O bonds [35], which can no further be connected through these oxo-oxygen atoms. Consequently, in [(UO$_2$)(H$_2$O)(C$_2$O$_4$)]·2H$_2$O, the chains are isolated. In M[(UO$_2$)$_2$(OH)(C$_2$O$_4$)$_2$]·2H$_2$O, the chains are connected through equatorial hydroxyl oxygen atoms to build a two-dimensional arrangement. In a few cases, uranyl polyhedra are directly connected by the so-called cation–cation interaction [36] in which an oxo-oxygen atom of a uranyl ion is also an equatorial oxygen of another uranium polyhedra (Fig. 4a). In Bi(C$_2$O$_4$)OH, the connection between the $^1_\infty$[{Bi(OH)E}(OH)(C$_2$O$_4$)] chains uses a similar concept: the apical hydroxyl oxygen of a BiO$_6$E pentagonal bipyramids is also an equatorial oxygen of another BiO$_6$E bipyramid (Fig. 4b). In uranium(VI)-containing oxides, the U–O–U angles involving common oxo-oxygen atoms are close to 180°, while the Bi–O–Bi angles in Bi(C$_2$O$_4$)OH are reduced to 142.5(3)°, due to the hydroxyl nature of the common oxygen atom.

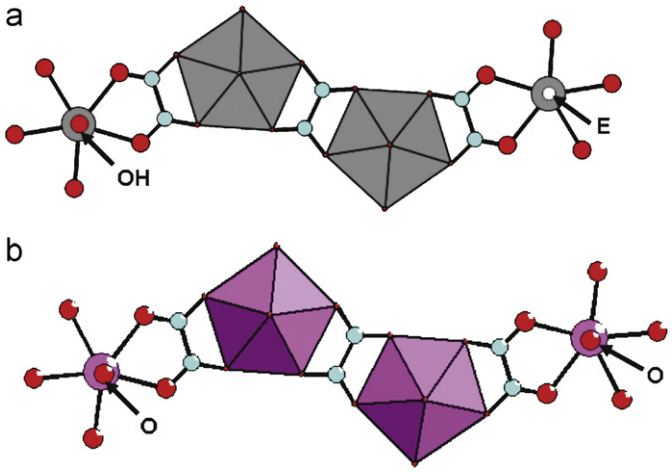

Fig. 3. Comparison between the bismuth oxalate $^1_\infty$[{Bi(OH)E}(OH)(C$_2$O$_4$)] chains built from {Bi(OH)E}O$_4$(OH) pentagonal bipyramids connected through bis-bidentate oxalate ions in Bi(C$_2$O$_4$)OH and the uranium oxalate and $^1_\infty$[{UO$_2$}(OH)(C$_2$O$_4$)] chains built from {UO$_2$}O$_4$(OH) pentagonal bipyramids connected through bis-bidentate oxalate ions in the compounds M[{UO$_2$}$_2$(OH)(C$_2$O$_4$)$_2$]·2H$_2$O, M = NH$_4^+$, Na$^+$, K$^+$ [32–34].

3.2. Thermal decomposition

During the synthesis of bismuth titanate, Umabala et al. [5] studied the thermal decomposition of a mixture of Bi(C$_2$O$_4$)OH and TiO(OH)$_2$·H$_2$O. A weight loss corresponding to an exothermic peak at 316 °C was attributed to the Bi(C$_2$O$_4$)OH decomposition into Bi$_2$O$_3$. A small endothermic peak at 740 °C was ascribed to the α-Bi$_2$O$_3$ to δ-Bi$_2$O$_3$ phase transition. Our TGA/DTA experiments confirm these conclusions. The analysis of the evolved gas shows the simultaneous departure of H$_2$O and CO$_2$ during the mass loss, indicating simultaneous dehydration and oxalate decomposition (Fig. 5). Moreover, our DTA experiment reveals a small exothermic peak at 360 °C, which is accompanied with neither mass loss nor gas evolution. To explain this transition, high-temperature X-ray diffraction (HTXRD) experiments were undertaken and are reported in Fig. 6. They confirm the disappearance of the Bi(C$_2$O$_4$)OH X-ray diffraction pattern, which occurs at about 250 °C, instead of the previously reported 316 °C. The temperature difference is probably due to the kinetic difference between thermal analysis and HTXRD experiments (heating rate 11° h^{-1} for HTXRD compared to 300° h^{-1} for TGA/TDA). In fact, the X-ray pattern of the obtained compound does not correspond to α-Bi$_2$O$_3$ but astonishingly to the meta-stable β-Bi$_2$O$_3$ (quadratic) form, which is generally observed between 650 and 300 °C during slow cooling of the high-temperature δ-Bi$_2$O$_3$ phase or melted bismuth oxide [37]. The HTXRD pattern at 300 °C indicates the β-Bi$_2$O$_3$ transition to the stable α-Bi$_2$O$_3$ (monoclinic) phase, which corresponds to the small exothermic peak at 360 °C observed during thermal analysis. Finally, the transition of α-Bi$_2$O$_3$ to the high-temperature δ-Bi$_2$O$_3$ cubic phase is observed at 730 °C. Thus the complete transformation is: Bi(C$_2$O$_4$)OH → β-Bi$_2$O$_3$ → α-Bi$_2$O$_3$ → δ-Bi$_2$O$_3$.

4. Conclusion

The slow diffusion through a gel allowed the growth of good-quality crystals of Bi(C$_2$O$_4$)OH. Single-crystal structure analysis reveals the stereochemical activity of the Bi^{3+} lone pair (E) and an original BiO$_6$E pentagonal bipyramid is observed. The connection of the pentagonal bipyramids by hydroxyl oxygen atoms leads to an inorganic arrangement further connected through bis-bidentate

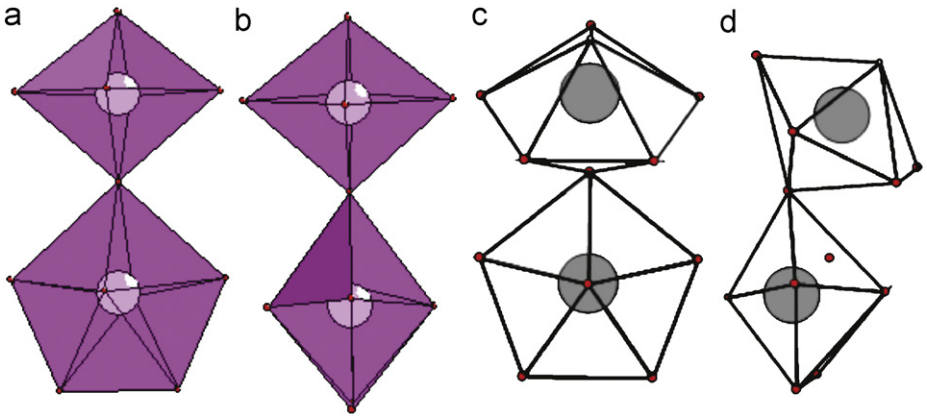

Fig. 4. Illustration of the cation–cation interaction between uranyl units in M(UO$_2$)$_4$(VO$_4$)$_3$ (M = Li, Na) [38] (a and b) and bismuth polyhedron in Bi(C$_2$O$_4$)OH. The hydroxyl oxygen is axial for one BiO$_4$(OH)$_2$E pentagonal bipyramid and equatorial for one another (c). The hydroxyl nature of the shared oxygen leads to a reduction of the M–O–M angle from 180° for M = U to 142.5(3)° for M = Bi (d).

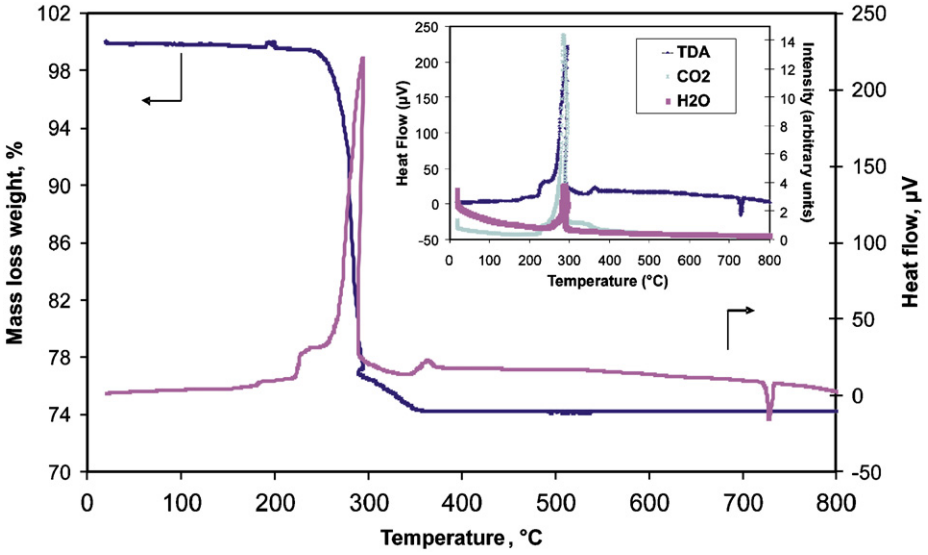

Fig. 5. TGA/TDA/MS curves for $Bi(C_2O_4)OH$ under flowing air (heating rate: 5°/min).

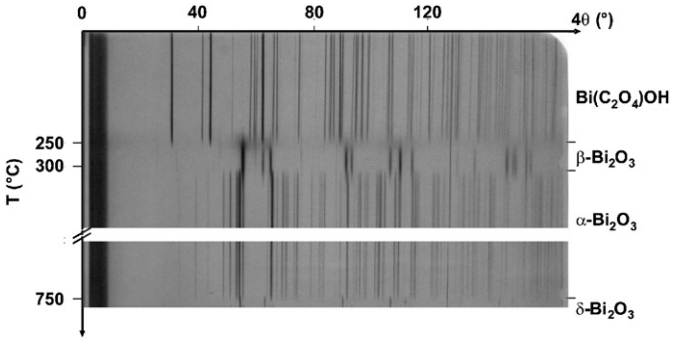

Fig. 6. HTXRD Guinier–Lenné pattern for $Bi(C_2O_4)OH$ under air (heating rate: ~0.2°/min).

oxalate ions. The thermal decomposition leads to the stabilization of the quadratic β-Bi_2O_3 phase between 310 and 360 °C. Syntheses and characterization of other bismuth-containing oxalates are in progress.

Acknowledgments

The "Fonds Européen de Développement Régional (FEDER)", "CNRS", "Région Nord Pas-de-Calais" and "Ministère de l'Education Nationale de l'Enseignement Supérieur et de la Recherche" are acknowledged for fundings of X-ray diffractometers.

The crystallographic data have been deposited and can be obtained through the FIZ data bank, on quoting the depository no. CSD-419313.

References

[1] C. Mao, L. Zhou, X. Sun, X. Wu, Physica C 281 (1997) 35.
[2] B.M. Popa, A. Totovana, L. Popescu, N. Dragan, M. Zaharescu, J. Eur. Ceram. Soc. 18 (1998) 1265.
[3] B.M. Popa, J.M. Calderon-Moreno, M. Zaharescu, J. Eur. Ceram. Soc. 20 (2000) 2773.
[4] M. Villegas, C. Moure, J.F. Fernandez, P. Duran, Ceram. Int. 22 (1996) 15.
[5] A.M. Umabala, M. Suresh, A.V. Prasadarao, Mater. Lett. 44 (2000) 175.
[6] T. Thongtem, S. Thongtem, Ceram. Int. 30 (2004) 1463.
[7] S.P. Gaikwad, S.B. Dhesphande, Y.B. Khollam, V. Samuel, V. Ravi, Mater. Lett. 58 (2004) 3474.
[8] S.R. Dhage, R. Pasricha, A. Vadival Murugan, V. Ravi, Mater. Chem. Phys 98 (2006) 344.
[9] S.P. Gaikwad, S.R. Dhage, H.S. Potdar, V. Samuel, V. Ravi, J. Electroceram. 14 (2005) 83.
[10] M. Devillers, F. De Smet, O. Torions, Thermochim. Acta 260 (1995) 165.
[11] M. Devillers, O. Torions, L. Cadus, P. Ruiz, B. Delmon, J. Solid State Chem. 126 (1996) 152.
[12] U. Kolitsch, Acta Crystallogr. C 59 (2003) 501.
[13] L. Tortet, O. Monnereau, P. Roussel, P. Conflant, J. Phys. 118 (2004) 43.
[14] G. Polla, R.F. Baggio, E. Manghiand, P.K. De Perazzo, J. Cryst. Growth 67 (1984) 68.
[15] L. Tortet, O. Monnereau, P. Conflant, G. Vacquier, Ann. Chim. Sci. Mater. 32 (2007) 69.
[16] [a] B. Chapelet-Arab, G. Nowogrocki, F. Abraham, S. Grandjean, J. Solid State Chem. 177 (2004) 4269;
[b] B. Chapelet-Arab, S. Grandjean, G. Nowogrocki, F. Abraham., J. Solid State Chem. 178 (2005) 3046;
[c] B. Chapelet-Arab, S. Grandjean, G. Nowogrocki, F. Abraham, J. Solid State Chem. 178 (2005) 3055;
[d] B. Chapelet-Arab, L. Duvieubourg, F. Abraham, G. Nowogrocki, S. Grandjean, J. Solid State Chem. 179 (2006) 4003.
[17] SAINT plus Version 6.22, Bruker Analytical X-ray Systems, Madison, WI, 2001.
[18] G.M. Scheldrick, SADABS, Bruker-Siemens area detector absorption and other correction, Version 2.03, Goetingen, Germany, 2001.
[19] V. Petricek, M. Dusek, L. Palatinus, JANA2000, Institute of Physics, Praha, Czech Republic, 2005.
[20] A. Altomare, G. Cascaro, G. Giacovazzo, A. Guargliardi, M.C. Burla, G. Polidori, M. Gamalli, J. Appl. Crystallogr. 27 (1994) 135.
[21] C.W. Haigh, Polyhedron 14 (1995) 2871.
[22] R. Enjalbert, S. Sorokina, A. Castro, J. Galy, Acta Chem. Scand. 49 (1995) 813.
[23] U. Heinl, P. Hinse, R. Mattes, Z. Anorg. Allg. Chem. 627 (2001) 2173.
[24] G. Vanhoyland, A. Le Bail, J. Mullens, L.C. Van Poucke, Inorg. Chem. 43 (2004) 785.
[25] X. Yu, H. Zhang, Y. Cao, Z. Hu, Y. Chen, Z. Wang, J. Solid State Chem. 179 (2006) 3095.
[26] E. Morin, G. Wallez, S. Jaulmes, J.C. Couturier, M. Quarton, J. Solid State Chem. 137 (1998) 283.
[27] A. Gleizes, J. Galy, J. Solid State Chem. 30 (1979) 23.
[28] N. Henry, M. Evain, P. Deniard, S. Jobic, O. Mentré, F. Abraham, J. Solid State Chem. 176 (2003) 127.
[29] N. Henry, O. Mentré, F. Abraham, E.J. MacLean, P. Roussel, J. Solid State Chem. 179 (2006) 3087.
[30] L. Duvieubourg, G. Nowogrocki, F. Abraham, S. Grandjean, J. Solid State Chem. 178 (2005) 3437.
[31] N.C. Jayadevan, D.M. Chackraburtty, Acta Crystallogr. B 28 (1972) 3178.
[32] M.Yu. Artem'eva, Yu.N. Mikhailov, Yu.E. Gorbunova, L.B. Serezhkin, V.N. Serezhkin, Zh. Neorg. Khim. 48 (2003) 1473.
[33] P. Thuéry, Polyhedron 26 (2007) 101.
[34] P.A. Giesting, P.C. Burns, N.J. Porter, Mater. Res. Soc. Proc. 893 (200-) 1.11.
[35] P.C. Burns, Can. Mineral. 43 (2005) 1839.
[36] N.N. Krot, M.S. Grigoriev, Russ. Chem. Rev. 73 (2004) 89.
[37] (a) P. Shuk, H.-D. Wiemhöfer, U. Guth, W. Göpel, M. Greenblatt, Solid State Ionics 89 (1996) 179;
(b) M. Drache, P. Roussel, J.P. Wignacourt, Chem. Rev. 107 (2007) 80.
[38] S. Obbade, C. Dion, M. Rivenet, M. Saadi, F. Abraham, J. Solid State Chem. 177 (2004) 2058.